MEG-Measured Visually Induced Gamma-Band Oscillations in Chronic Schizophrenia: Evidence for Impaired Generation of Rhythmic Activity in Ventral Stream Regions

Tineke Grent-'t-Jong[6*], Ph.D., Rivolta Davide[1,2,3*], Ph.D., Sauer Andreas[1,2], M.Sc., Grube, Michael[7], M.D., Singer Wolf[1,2,4], M.D., Ph.D., Wibral Michael[5], Ph.D. & Peter J. Uhlhaas[1,2,6], Ph.D.

1. Department of Neurophysiology, Max Planck Institute for Brain Research, Frankfurt am Main, 60528, Germany.

2. Ernst Strüngmann Institute (ESI) for Neuroscience in Cooperation with Max Planck Society, Frankfurt am Main, 60528, Germany

3. School of Psychology, University of East London (UEL), London, United Kingdom.

4. Frankfurt Institute for Advanced Studies (FIAS), Johann Wolfgang Goethe University, Frankfurt am Main, Germany.

5. MEG Unit, Brain Imaging Centre (BIC), Johann Wolfgang Goethe University, Frankfurt am Main, 60529, Germany.

6. Institute of Neuroscience and Psychology, University of Glasgow, Glasgow, United Kingdom.

7. Department of Psychiatry and Psychotherapy – Psychosomatics, Municipal Clinic, Frankfurt am Main, 65929, Germany.

* Shared first authorship

Running title: Reduced gamma-band oscillations in Schizophrenia

Number of Pages: 32

Number of Figures: 5

Number of Tables: 4

Number of words (Abstract): 247

Correspondence to:

Dr. Tineke Grent-'t-Jong,

Institute of Neuroscience and Psychology

University of Glasgow

Hillhead Street 58

Glasgow, G12 8QB

E-Mail: tineke.grent@glasgow.ac.uk

Tel: 0044-141-3305047

Fax: 0044-141-3304606

Abstract

Background: Gamma-band oscillations are prominently impaired in schizophrenia, but the nature of the deficit and relationship to perceptual processes is unclear.

Methods: 16 patients with chronic schizophrenia (ScZ) and 16 age-matched healthy controls completed a visual paradigm while magnetoencephalographic (MEG) data was recorded. Participants had to detect randomly occurring stimulus acceleration while viewing a concentric moving grating. MEG data were analyzed for spectral power (1-100 Hz) at sensor- and source-level to examine the brain regions involved in aberrant rhythmic activity, and for contribution of differences in baseline activity towards the generation of low- and high-frequency power.

Results: Our data show reduced gamma-band power at sensor level in schizophrenia patients during stimulus processing while alpha-band and baseline spectrum were intact. Differences in oscillatory activity correlated with reduced behavioral detection rates in the schizophrenia group and higher scores on the "Cognitive Factor" of the Positive and Negative Syndrome Scale**.** Source reconstruction revealed that extra-striate (fusiform/lingual gyrus), but not striate (cuneus), visual cortices contributed towards the reduced activity observed at sensor-level in ScZ patients. Importantly, differences in stimulus-related activity were not due to differences in baseline activity.

Conclusions: Our findings highlight that MEG-measured high-frequency oscillations during visual processing can be robustly identified in ScZ. Our data further suggest impairments that involve dysfunctions in ventral stream processing and a failure to increase gamma-band activity in a task-context. Implications of these findings are discussed in the context of current theories of cortical-subcortical circuit dysfunctions and perceptual processing in ScZ.

1. Introduction

Recent evidence has highlighted the contribution of impaired perceptual processing towards behavioural and physiological deficits in schizophrenia (ScZ). This is supported through data from anatomy (Selemon et al., 1995), physiology (Rivolta et al, 2014; Sun et al., 2013; Grützner et al., 2013; Krishnan et al., 2005; Butler et al., 2007) and psychophysics (Butler et al., 2008; Uhlhaas and Silverstein, 2005; Uhlhaas and Mishara, 2007), which has highlighted that the earliest stages of auditory and visual processing might be compromised. As a result, dysfunctions in "higher" cortical regions that support more complex cognitive processes involved in executive functions and social cognition could be essentially due to deficits in bottom-up driven sensory activity (Javitt, 2009).

Abnormalities in rhythmic activity at low and high frequencies could provide a mechanism for dysfunctional perception in ScZ (Tan et al., 2013). Rhythmic activity at gamma-band frequencies has been shown to systematically correlate with stimulus parameters, such as contrast, size, or retinal location (Muthukumaraswamy and Singh, 2013). This has led to the conclusion that gamma-band activity may essentially be involved in feed-forward propagation of sensory activity along the visual hierarchy (Michalareas et al., 2016) which is consistent with the laminar expression profile (Markov et al., 2014). More specifically, high frequency oscillations occur predominantly in granular layers 3 and 4, while alpha (8-12 Hz)/beta (13-30 Hz) oscillations occur predominantly in infra-granular layers 5 and 6 (Bastos et al., 2015; van Kerkoerle et al., 2014). In addition to stimulus parameters, the amplitude and frequency of high-frequency oscillations in visual cortices can also be influenced by central states, such as attention. Initial evidence for this was provided by Fries and colleagues (Fries et al., 2001) who showed that 35-90 Hz activity in macaque visual area V4 strongly increased when behaviourally relevant stimuli were within the focus of attention. Moreover, attentional states and expectancy strongly impacts on activity prior to

the onset of stimulus (Beck and Kastner, 2009; Corbetta and Shulman, 2002). Stimulus expectation is typically expressed in a decrease of power in the lower, in particular alpha-frequency range prior to stimulus onset and often predicts subsequent task performance (Thut et al., 2006, van Dijk et al., 2008). In contrast to lower frequencies, higher frequencies in the gamma-band range typically only increase in power shortly after the expected stimulus arrives (Bauer et al., 2014). Accordingly, it has been hypothesized that, across areas in the visual processing hierarchy, alpha-band oscillations are involved in feedback propagation of information flow while gamma-band activity are strongly involved in feed-forward mediated information processing of stimulus-related activity (Fries, 2015).

Several EEG/MEG-studies have provided preliminary evidence for the potential role of abnormal high-frequency oscillations in visual-perceptual deficits in ScZ (Spencer et al., 2008; Sun et al., 2013, Grützner et al., 2013). However, the underlying generators as well as the potential mechanisms remain unclear. One possibility is that impaired high-frequency oscillations in ScZ are the direct consequence of dysfunctions in neurobiological mechanisms that underlie the generation of rhythmic activity in sensory cortices (Tan et al., 2013). Gamma-band oscillations are critically dependent upon the balance between Excitation and Inhibition (E/I-balance) mediated by NMDA/AMPA-receptors and GABAergic interneurons in local circuits which determine the strength and duration of the oscillations (Wang and Buzsaki, 1996; Fuchs et al., 2007; Whittington and Traub, 1995; Carlen et al., 2012). In ScZ, there is extensive evidence for disturbance in these parameters (Uhlhaas and Singer, 2012) that include alterations in visual cortices, such as reductions in the mRNA of GAD67, an enzyme that synthesizes GABA (Hashimoto et al., 2003). Furthermore, Magnetic Resonance Spectroscopy (MRS)-measured reduction in GABA-levels was found to correlate with psychophysical impairment in orientation-specific surround suppression in ScZ patients (Yoon et al., 2010), suggesting a potential role in visual dysfunctions.

To address the possibility that visual cortices in ScZ are characterized by impairments in the generation of gamma-band oscillations and to elucidate potential correlations with impairments in alpha oscillations before and during stimulus processing, we employed a visual task that was designed to elicit robust high-frequency activity in the context of focused attention (Hoogenboom et al., 2006). Previous data showed excellent signal-to-noise ratio (SNR) for gamma-band oscillations and high reliability across measurements (Muthukumaraswamy et al., 2010). In combination with detailed source reconstruction of MEG-measured high-frequency oscillations, we expected novel insights into the contribution of brain areas and alpha oscillations towards impaired high-frequency oscillations in ScZ. Moreover, our analysis allowed the examination of alterations in rhythmic activity during the pre-stimulus baseline period, and its potential effects on subsequent task-induced activity. There is evidence suggesting a positive correlation between high pre-stimulus (baseline) alpha-band power over visual cortex and poor stimulus-detection performance (Romei et al., 2008, 2010). Accordingly, we analysed baseline and task induced oscillations at sensor-level and in virtual channels to examine this possibility.

2. Methods and materials

2.1 Participants

Sixteen chronic schizophrenia (ScZ) patients (6 females, mean age 34 ± 10.6 years [standard deviation: STDEV]) were recruited from the in- and outpatients units of the Dept. of Psychiatry, affiliated hospital Hoechst, Frankfurt, Germany. All ScZ-patients met DSM-IV criteria for ScZ and were on stable antipsychotic treatment. Sixteen age-matched healthy controls (6 females, mean age 31 ± 8.0 years) were recruited from the local community. The study was carried out according to the Declaration of Helsinki and approved by the ethical committees of the Goethe-University Frankfurt. After complete description of the study to the

participants, written informed consent was obtained. DSM-IV diagnosis of ScZ was established with the SCID Interview (Saß et al., 2003), by thorough chart review and in consultation with the treating psychiatrists. Patients and controls were excluded if they had any neurological or ophthalmologic disorders that might have affected performance or if they met criteria for alcohol or substance dependence within the last month. Current psychopathology was assessed with the Positive and Negative Syndrome Scale (PANSS) and symptoms were grouped into five factors according to the model of Lindenmayer (Lindenmayer et al., 1995), including the factors "positive", "negative", "depression", "excitement" and "cognitive" (see Table 1).

2.2. Stimuli and task

The experimental paradigm adopted was modified after Hoogenboom et al. (2006). On each trial, participants were shown a circular sine wave grating at central screen fixation that contracted towards the fixation point (visual angle: 5°; spatial frequency: 2 cycles per degree; contrast: 100%). Subjects had one second to press the response button with their right index finger when the stimulus increased velocity (velocity step to 2.2 °/s), which could randomly occur between 500 ms and 3000 ms post stimulus onset (10% of the trials were catch trials in which no acceleration occurred). After a response was given (or in catch trials 3000 ms after stimulus onset) a visual feedback was shown (Figure 1). Each subject completed eight blocks of 60 trials. An LCD projector located outside of the magnetically shielded room of the MEG was used to project the stimuli onto the screen via two front-silvered mirrors. Stimulus presentation was controlled by the Presentation software package (Neurobehavioral Systems).

2.3 MEG data acquisition

MEG data were acquired using a 275-sensors whole-head system (Omega 2005, VSM MedTech Ltd, BC, Canada) with a sampling rate of 6000 Hz in a synthetic third order axial gradiometer configuration. Participants' head movement was recorded before and after each run, using coils placed on the nasion and 1 cm anterior to the tragus of the left and right hear.

2.4 Anatomical (MRI) data acquisition

A high-resolution anatomical MRI scan was acquired for each participant using a 3D magnetization-prepared rapid-acquisition gradient echo sequence (160 slices; voxel size: 1x1x1 mm; FOV: 256 mm; TR: 2300 ms; TE: 3.93 ms). During the structural scan, vitamin E pills were applied to the nasion and 1 cm anterior to the tragus of the right and left ear to allow for co-registration of the MEG and MRI data. Scanning was performed with a 3-Tesla Siemens Trio scanner.

2.5 MEG data analysis

All MEG analyses were performed with Fieldtrip (Oostenveld et al., 2011). Trials were defined as non-overlapping data segments starting 1000 ms before stimulus onset until 1800 ms post-stimulus onset. Power line fluctuations were removed by using a discrete 50 Hz Fourier transform filter (including the first two harmonics). Trials containing muscle artifacts or sensor (SQUID) jumps were discarded using semi-automatic artifact rejection routines. Subsequently, artifacts due to eye blinks, eye movements, and the heart-beat signal were removed using ICA-decomposition and removal strategies. Furthermore, data were down-sampled to 300 Hz. Preprocessing and cleaning of the data left statistically identical number of trials for further analyses for both groups of participants (Table 2).

2.5.1 Sensor-level analysis

Time frequency analyses at sensor-level were performed for planar-orientation transformed MEG data (Bastiaansen and Knösche, 2000), which simplifies the interpretation of the sensor data, as with planar gradients the maximal signal is located above the source (Hämäläinen et al., 1993). Time-frequency power representations (TFRs) were computed based on a sliding window Fourier transform approach, with a step-size of 50 ms across the length of the epochs. Power of all frequencies between 1-100 Hz were estimated based on 4 seconds of padded data, using a frequency resolution of 1 Hz, and multiplying the data with a Hanning taper before power estimation.

Power changes across time were subsequently expressed as absolute changes from baseline (-500-0 ms) power. An additional Fast Fourier Transformation (FFT) was run for frequencies between 1-100 Hz (step-size 1 Hz, Hanning tapered) on smaller data segments, averaged across 500 ms of baseline period (-500-0 ms) and 500 ms of stimulus processing period (500-1000 ms). These FFT data were used to determine individual peak frequencies in the alpha (using baseline data) and gamma range (assessed from the absolute difference between the active and baseline FFT data).

2.5.2 Sensors- level statistics

Significant differences between healthy controls and ScZ patients in stimulus-driven alpha (8-13 Hz) and gamma (47-67 Hz) power changes from baseline were assessed using independent samples t-tests in cluster-based non-parametric permutation statistics (Maris and Oostenveld, 2007). We used 2000 permutations for bootstrapping and assumed significant group differences when the computed *p*-value (taken from the proportion of random partitions that showed larger test statistics then the observed ones) was smaller than the critical alpha-level of 0.05. A minimum cluster of 2 adjacent sensors was required before a cluster of sensors was accepted as different between both groups, correcting for multiple

comparisons. Statistical tests were computed for two windows of interest: an early (250-750 ms) and a later (750-1250 ms) time window during stimulus processing, in order to track changes over time.

2.5.3 Source-level analysis and statistics

Source estimation of oscillatory activity changes was performed using the dynamic imaging of coherent sources (DICS) beamforming approach (Gross et al., 2001). Participant-specific source power values were normalized to a three-dimensional template grid (5 mm spacing) in Montreal Neurological Institute (MNI) coordinates, co-registered to the MEG coordinates system specific to the participant's head. Sources were estimated for baseline activity (-500-0 ms), the early (250-750 ms) and late (750-1250 ms) stimulus processing windows of interest, separately for alpha (individual peak frequency ± 2 Hz) and gamma (individual peak frequency ± 10 Hz) power absolute changes from baseline. Source activity for the early and late window was estimated by subtracting the source power estimates of the baseline window from the source power estimates of each time window (i.e., absolute change). Source activity data were analyzed statistically using independent samples t-tests in a cluster-based permutation approach with 2000 permutations. Clusters of differential activity between controls and patients were assumed significant at the first-order level when the independent permutation-based *t*-values exceeded the critical t-value (2.13) for our number of independent observations (i.e. uncorrected for multiple comparisons).

2.5.4 Virtual channel analysis and statistics

To further investigate potential group differences at a smaller spatial scale, we selected three regions of interest (ROIs), cuneus, lingual and fusiform gyrus, based on the grand-average group difference (Figure 3/4). Using an LCMV beamformer approach, we created ROI-

specific single-trial MEG time-series (i.e., virtual channel) data for each participant. These data were subsequently submitted to TFR analysis (similar parameters as original data), averaging the data from left and right hemisphere. Statistical differences between alpha (8-13 Hz) and gamma (47-67 Hz) activity within each ROI were then estimated across time for baselined data, accepting a minimum of 3 adjacent time points (total duration of 150 ms) as significant group differences.

2.6 Correlational analysis

Behavioural performance (accuracy and mean reaction time data), PANSS scores (all 5 factor scores) and early-window (250-750 ms) virtual channel alpha (8-13 Hz) and gamma (47-67 Hz) power data (data from all three ROIs: log10 transformed to increase linearity) extracted for 15 ScZ patients with available PANSS scores were submitted to Spearman's Rho correlational analysis. Statistical significance was assumed when the 2-tailed probability exceeded the critical α-level of 0.05.

3. Results

3.1. Behavioural Data

Performance on the moving grating task was different between the two groups (Table 2). Although ScZ patients and healthy controls (HC) were on average equally fast in responding, accuracy was significantly lower for the ScZ patients ($p = 0.001$).

3.2. Sensor-level data

3.2.1 Task-Induced activity

Time-frequency responses (TFRs) of sensor-level data (Figure 2A) revealed stimulus-induced increases in gamma and decreases in alpha band power, compared to baseline power, a

pattern that was present for both groups. Topographic distributions of the maximum power changes for both frequencies of interest were found mostly over visual cortical areas, with a slightly more medial location for the gamma-power increases and a slightly more lateral focus for the alpha-power decreases (Figure 2B).

Changes in gamma- and alpha-band power appeared to be of smaller in amplitude for ScZ patients than for controls. Cluster-based non-parametric permutation statistics (Table 3) confirmed significant group differences (HC > ScZ) for gamma power increases (47-67 Hz) over a cluster of posterior sensors (Figure 2D), for both the early (250-750 ms, $p < 0.02$) and later time window (750-1250 ms, $p < 0.01$). In addition, gamma power was significantly higher in controls than ScZ patients in a mid-frontal cluster, both early and later in time (early: $p < 0.04$, late: $p < 0.03$).

In contrast, alpha (8-13 Hz) power decreases during these two time windows were not significantly different between the two groups (Table 3). However, there were differences in the peak-frequency (Figure 2C & Table 2) with alpha peak frequencies being significantly lower for ScZ patients than for healthy controls ($p = 0.04$). In contrast, individual gamma peak frequencies were not significantly different between groups (Table 2). Because of these differences, subsequent source estimations (and source statistics) were performed on data selected around the individual peak frequencies (gamma peak ± 10 Hz, alpha peak ± 2 Hz) rather than using frequency ranges based on the group averages.

3.2.2 Baseline activity

In order to rule out that group differences were caused by baseline power differences, we also directly contrasted pure baseline power (averaged data from -500 ms pre-stimulus to stimulus onset) and non-baselined task induced power changes (averaged data between 500-1000 ms

post-stimulus onset) using FFT-transformed sensor data. No significant differences in alpha/gamma-band power were observed (Figure 2C).

3.3. Source-level data

3.3.1 Task-Effects

Gamma (~47-67 Hz) power changes from baseline were localized to parietal, occipital, inferior and mid temporal cortex, angular gyrus, posterior cingulum and the thalamus. Alpha (~8-13 Hz) power changes were localized mostly to parietal, occipital and mid temporal cortex, with additional areas for the schizophrenia group including precentral gyrus, mid cingulate cortex, supplementary motor areas, superior frontal cortex, caudate and the thalamus (Figure 3A/3B).

Statistical analysis (Table 3) showed that for task-induced gamma power changes (Figure 3C), group differences were most pronounced over fusiform gyrus, inferior and mid occipital and temporal areas and in the left superior frontal cortex ($p < 0.05$, $t > 2.13$; uncorrected). For alpha power, significant group differences were only found for the later time window (Table 3), including clusters in the fusiform gyrus, lingual gyrus, and inferior and mid occipital and temporal areas and over left mid superior frontal gyrus ($p < 0.05$, $t > 2.13$; uncorrected).

3.3.2 Virtual Channels

To further investigate the modulation of alpha/gamma-band oscillations in visual areas, virtual channel were computed for the left and right fusiform gyrus, lingual gyrus and cuneus, areas indicated by the grandaverage source differences (Figure 3).

Alpha-band power was significantly reduced in ScZ patients in the fusiform gyrus while no differences were observed in the lingual gyrus and cuneus (Figure 4, Table 3). In

contrast, significant differences in gamma power increases were revealed in the lingual gyrus and to some extent also in the fusiform gyrus at early latencies, but no such differences were seen in the cuneus (Table 3). Surprisingly, the groups did not differ in their alpha or gamma responses in early (striate) visual cortex (cuneus). Finally, as with the above reported whole-head sensor- and source-level data, virtual-channel data reconstructed for the three occipital ROIs did no show statistical differences in baseline activity.

3.4. Correlations with behavioural performance and symptom severity

Spearman's Rho correlations between behavioural performance (accuracy and mean reaction times), PANSS Factors and source-reconstructed alpha- and gamma-band activity (virtual channel data: 250-750 ms) for 15 ScZ patients revealed strong positive correlations between behavioural accuracy levels and alpha- and gamma-power changes in each of the three ROIs (see Table 4). In addition, significant negative correlations were found between the oscillatory activity in the three ROIs and the scores on the Cognitive Factor of the PANSS.

4. Discussion

The current findings demonstrate that visual cortices in ScZ are involved in the failure to generate optimal amplitudes of gamma-band oscillations in ventral stream occipital areas. Previous findings with EEG and MEG reported reductions in the amplitude and phase of high-frequency oscillations during visual tasks at illness-onset and in chronic ScZ (Tan et al., 2013; Spencer et al., 2008, Sun et al, 2013, Grützner et al., 2013). However, because of the potential contribution of distinct and distributed sources towards fluctuations in sensor-measured EEG/MEG-data, these data do not allow reliable insights into the origin of gamma-band dysfunctions. This problem is highlighted in this study by an unexpected absence of significant sensor-level alpha-power effects and unexpected shifts (slightly more anterior) in

the topography of significant changes in gamma-band power between the groups than expected based on visual inspection of the data (Figure 2A & B vs. D). The more reliable MEG-informed beamforming of task-induced stimulus-processing activity, however, revealed that in ScZ extra-striate areas of the ventral stream were characterized by pronounced reductions in alpha and gamma-band amplitude, whereas striate areas were not.

The current data are consistent with empirical findings and formulations in the literature that have highlighted aberrant neural responses in visual cortices that could underlie deficits in sensory registration and/or propagation of feedforward-mediated information in ScZ (Tan et al., 2013; Javitt, 2015, Butler et al., 2008). In the visual cortex of ScZ patients, reduced synaptic contacts (Selemon et al., 1995) as well as reduced markers of interneuron activity have been observed (Hashimoto et al., 2008), which together could provide possible mechanisms for the observed reductions in high-frequency oscillations as these are critically dependent upon rhythmic inhibition of large number of pyramidal cells (Whittington and Traub, 2003).

The reductions in gamma-band oscillations in ScZ patients in the current study were most prominent in the lingual gyrus and fusiform gyrus while the gamma activity in the cuneus was intact. Both the fusiform gyrus and the lingual gyrus are considered part of the ventral stream which is crucially involved in object recognition. Moreover, as gamma-band activity was also unimpaired in early visual cortex, the most parsimonious interpretation of the MEG data would favour a deficit in ventral stream generators. This conclusion is consistent with recent data that highlight that reductions in P1 amplitude may mostly involve impaired contributions from extra-striate cortex while initial afferent activity (through magnocellular pathways) to early visual cortex is intact in ScZ patients (Lalor et al., 2012; for different findings, however, see e.g., Butler et al., 2008; Javitt et al., 2009, 2015).

One important finding with wider implications for the interpretation of circuit dysfunctions in ScZ is the absence of differences in gamma-band power during the baseline period in our data. Several studies showed elevated spectral power during the pre-stimulus period (Hirano et al., 2015) as well as in resting-state recordings (Kikuchi et al., 2011). As ongoing neural activity strongly impacts the ability to process incoming sensory information and potentially impacts estimates of post-stimulus activity in EEG/MEG-analyses, further data are required to exclude the possibility that aberrant stimulus-induced high-frequency oscillations in ScZ are related to impaired spontaneous gamma-band activity. The latter finding would also be consistent with evidence from the effects of NMDA-R antagonists which lead to increase in spontaneous high-frequency power (Rivolta et al., 2015) and thus to a decrease in SNRs in circuits during sensory processing (Anticevic et al., 2012).

Overall, our analyses of both sensor- and source-space derived estimates of baseline gamma-band power do not support this perspective. Instead, the current findings favour an interpretation that highlights a failure of visual cortices to generate high-frequency oscillations in a task-context. As a result, these findings may provide stronger support for impairments in GABAergic neurotransmission, as a potential candidate mechanism for the observed in reductions in high-frequency activity (Lewis et al., 2005; Sohal et al., 2009).

Alpha, like gamma activity, appeared to be more impaired in extra-striate than striate cortex. Alpha generators have been found in different layers of both striate and extra-striate visual areas (Bollimunta et al., 2008, 2011; Mo et al., 2011; Haegens et al., 2015; van Kerkoerle et al., 2014), and are known to be modulated in activity by both cortico-cortical and recurrent thalamo-cortical (TC) communication (Steriade et al., 1990), influenced by thalamic nuclei such as the lateral geniculate nucleus (LGN), the pulvinar nucleus, and the thalamic reticular nucleus (TRN). Evidence is growing that these different thalamic nuclei play different roles in sensory information processing, both spatially (i.e., across the visual

hierarchy) and temporally (i.e., during early feedforward and later feedback processing). Given the transient nature of our cuneus-driven alpha-power responses, known driving granular input to striate cortex from the LGN (Jones, 2001, 2002; Hughes et at., 2004; Lorincz et al., 2008; Bollimunta et al., 2011), and reported inability of the TRN to interfere with the generation of sensory-evoked potentials (Jasper, 1949), the current results suggest an intact functioning of the afferent stimulus-driven alpha activity relayed through the direct retina-geniculate-striate cortex pathway to the cuneus in our schizophrenia patients.

In contrast to striate projections, thalamic projections to extra-striate cortex have been shown to originate mostly from non-specific thalamic nuclei and from higher order nuclei such as the pulvinar, driven to a large extent by cortico-fugal input to the TRN (Sherman and Guillery, 2002). Selective contributions from extra-striate cortex and pulvinar, but not from striate cortex and LGN, has been reported recently for pattern motion processing (Villeneuve et al., 2012). Moreover, LGN and V1 were selective only for the spatial frequency characteristics of the stimuli, not for motion processing. Thus, it is possible that our sustained lingual and fusiform gyrus alpha (and gamma) activity represent the selective attentional processing of the speed of the inward motion of the grating. Extra-striate activity is likely influenced by top-down modulation from other visual areas, the frontal-parietal attention network, and TC input from the pulvinar (Saalman et al., 2012). Thus, in ScZ patients, diminished top-down modulation of extra-striate alpha activity might in part explain the lack of proper feedforward-propagation of gamma activity due to weaker feedback cortico-cortical and TC signals to striate cortex.

With respect to our statistical results, although our whole-head between-group independent t-tests for the source reconstructions of alpha- and gamma-band power did not survive the corrections for multiple comparisons, we would like to argue that this does not preclude potential group differences in a subset of areas across the cortical processing

hierarchy that showed rather clear group differences (see Figure 3A/B, right panels), differences that actually could explain our significant sensor-level gamma-band power. Our relatively small sample size coupled with an expected limited scope of effects on the spatial scale (i.e., expected primary over occipital cortex) does not fit the cluster-based data-driven statistical approach very well (see for a discussion on this topic: Maris, 2011). The more hypothesis-driven ROI analyses demonstrate this point clearly by revealing significant group differences in areas indicated by the first-order source statistics (uncorrected results presented in Figure 3C).

Finally, our data also potentially suggest a link between aberrant rhythmic activity and impaired behavior and cognition in ScZ. Specifically, we found highly significant correlations between behavioural accuracy, the factor "Cognitive" of the PANSS and visual-cortex oscillatory alpha- and gamma-band responses in chronic ScZ patients. These findings are consistent with previous theoretical (Philipps and Silverstein, 2003) and empirical data (Spencer et al., 2004, Uhlhaas and Silverstein, 2005; Uhlhaas et al., 2006), which have highlighted a close correspondence between clinical disorganization, visual dysfunctions and aberrant high-frequency oscillations. Our data go beyond these findings through demonstrating correlations across these measures in task-related visual regions, thus adding important evidence for the functional relevance of changes in neural oscillations in ScZ.

In summary, our data provide a novel perspective on low- and high- frequency oscillations during visual processing in ScZ. Specifically, our findings indicate an impaired generation of high-frequency activity in upstream/ventral regions of the visual cortex in ScZ in the context of decreased suppression of low-frequency activity, which could be linked to more severe illness status. Potential limitations for these conclusions are relatively small sample size as well as the fact that all ScZ patients were on anti-psychotic medication at the time of testing. However, the current results are in line with our earlier findings of

significantly reduced visual gamma-band oscillations in un-medicated first-episode ScZ patients (Sun et al., 2013).

References

Anticevic, A., Gancsos, M., Murray, J.D., Repovs, G., Driesen, N.R., Ennis, D.J., Niciu, M.J., Morgan, P.T., Surti, T.S., Bloch, M.H., Ramani, R., Smith, M.A., Wang, X.J., Krystal, J.H., Corlett, P.R., 2012. NMDA receptor function in large-scale anticorrelated neural systems with implications for cognition and schizophrenia. Proc.Natl.Acad.Sci.U.S.A 109, 16720-16725.

Bastiaansen, M.C., Knösche, T.R., 2000. Tangential derivative mapping of axial MEG applied to event-related desynchronization research. Clin.Neurophysiol. 111, 1300-1305.

Bastos, A.M., Vezoli, J., Bosman, C.A., Schoffelen, J.M., Oostenveld, R., Dowdall, J.R., De, W.P., Kennedy, H., Fries, P., 2015. Visual Areas Exert Feedforward and Feedback Influences through Distinct Frequency Channels. Neuron 85, 390-401.

Bauer, M., Stenner, M.P., Friston, K.J., Dolan, R.J., 2014. Attentional modulation of alpha/beta and gamma oscillations reflect functionally distinct processes. J.Neurosci. 34, 16117-16125.

Beck, D.M., Kastner, S., 2009. Top-down and bottom-up mechanisms in biasing competition in the human brain. Vision Res. 49, 1154-1165.

Bollimunta, A., Chen, Y., Schroeder, C.E., Ding, M., 2008. Neuronal mechanisms of cortical alpha oscillations in awake-behaving macaques. J.Neurosci. 28, 9976-9988.

Bollimunta, A., Mo, J., Schroeder, C.E., Ding, M., 2011. Neuronal mechanisms and attentional modulation of corticothalamic alpha oscillations. J.Neurosci. 31, 4935-4943.

Butler, P.D., Martinez, A., Foxe, J.J., Kim, D., Zemon, V., Silipo, G., Mahoney, J., Shpaner, M., Jalbrzikowski, M., Javitt, D.C., 2007. Subcortical visual dysfunction in schizophrenia drives secondary cortical impairments. Brain 130, 417-430.

Butler, P.D., Silverstein, S.M., Dakin, S.C., 2008. Visual perception and its impairment in schizophrenia. Biol.Psychiatry 64, 40-47.

Carlen, M., Meletis, K., Siegle, J.H., Cardin, J.A., Futai, K., Vierling-Claassen, D., Ruhlmann, C., Jones, S.R., Deisseroth, K., Sheng, M., Moore, C.I., Tsai, L.H., 2012. A critical role for NMDA receptors in parvalbumin interneurons for gamma rhythm induction and behavior. Mol.Psychiatry 17, 537-548.

Corbetta, M., Shulman, G.L., 2002. Control of goal-directed and stimulus-driven attention in the brain. Nat.Rev.Neurosci. 3, 201-215.

Fries, P., Reynolds, J.H., Rorie, A.E., Desimone, R., 2001. Modulation of oscillatory neuronal synchronization by selective visual attention. Science 291, 1560-1563.

Fries, P., 2015. Rhythms for Cognition: Communication through Coherence. Neuron 88, 220-235.

Fuchs, E.C., Zivkovic, A.R., Cunningham, M.O., Middleton, S., Lebeau, F.E., Bannerman, D.M., Rozov, A., Whittington, M.A., Traub, R.D., Rawlins, J.N., Monyer, H., 2007. Recruitment of parvalbumin-positive interneurons determines hippocampal function and associated behavior. Neuron 53, 591-604.

Gross, J., Kujala, J., Hamalainen, M., Timmermann, L., Schnitzler, A., Salmelin, R., 2001. Dynamic imaging of coherent sources: Studying neural interactions in the human brain. Proc.Natl.Acad.Sci.U.S.A 98, 694-699.

Grützner, C., Wibral, M., Sun, L., Rivolta, D., Singer, W., Maurer, K., Uhlhaas, P.J., 2013. Deficits in high- (>60 Hz) gamma-band oscillations during visual processing in schizophrenia. Front Hum.Neurosci. 7, 88.

Haegens, S., Barczak, A., Musacchia, G., Lipton, M.L., Mehta, A.D., Lakatos, P., Schroeder, C.E., 2015. Laminar Profile and Physiology of the alpha Rhythm in Primary Visual, Auditory, and Somatosensory Regions of Neocortex. J.Neurosci. 35, 14341-14352.

Hashimoto, T., Volk, D.W., Eggan, S.M., Mirnics, K., Pierri, J.N., Sun, Z., Sampson, A.R., Lewis, D.A., 2003. Gene expression deficits in a subclass of GABA neurons in the prefrontal cortex of subjects with schizophrenia. J.Neurosci. 23, 6315-6326.

Hashimoto, T., Arion, D., Unger, T., Maldonado-Aviles, J.G., Morris, H.M., Volk, D.W., Mirnics, K., Lewis, D.A., 2008. Alterations in GABA-related transcriptome in the dorsolateral prefrontal cortex of subjects with schizophrenia. Mol.Psychiatry 13, 147-161.

Hämäläinen, M., Hari, R., Ilmoniemi, R.J., Knuutila, J., Lounasmaa, O.V., 1993. Magnetoencephalography - Theory, Instrumentation, and Applications to Noninvasive Studies of the Working Human Brain. Reviews of Modern Physics 65, 413-497.

Hirano, Y., Oribe, N., Kanba, S., Onitsuka, T., Nestor, P.G., Spencer, K.M., 2015. Spontaneous Gamma Activity in Schizophrenia. JAMA Psychiatry.

Hoogenboom, N., Schoffelen, J.M., Oostenveld, R., Parkes, L.M., Fries, P., 2006. Localizing human visual gamma-band activity in frequency, time and space. Neuroimage 29, 764-773.

Hughes, S.W., Lorincz, M., Cope, D.W., Blethyn, K.L., Kekesi, K.A., Parri, H.R., Juhasz, G., Crunelli, V., 2004. Synchronized oscillations at alpha and theta frequencies in the lateral geniculate nucleus. Neuron 42, 253-268.

Jasper, H., 1949. Diffuse projection systems: the integrative action of the thalamic reticular system. Electroencephalogr.Clin.Neurophysiol. 1, 405-419.

Javitt, D.C., 2009. When doors of perception close: bottom-up models of disrupted cognition in schizophrenia. Annu.Rev.Clin.Psychol. 5, 249-275.

Javitt, D.C., 2015. Neurophysiological models for new treatment development in schizophrenia: early sensory approaches. Ann.N.Y.Acad.Sci. 1344, 92-104.

Jones, E.G., 2001. The thalamic matrix and thalamocortical synchrony. Trends Neurosci. 24, 595-601.

Jones, E.G., 2002. Thalamic circuitry and thalamocortical synchrony. Philos.Trans.R.Soc.Lond B Biol.Sci. 357, 1659-1673.

Kikuchi, M., Hashimoto, T., Nagasawa, T., Hirosawa, T., Minabe, Y., Yoshimura, M., Strik, W., Dierks, T., Koenig, T., 2011. Frontal areas contribute to reduced global coordination of resting-state gamma activities in drug-naive patients with schizophrenia. Schizophr.Res. 130, 187-194.

Krishnan, G.P., Vohs, J.L., Hetrick, W.P., Carroll, C.A., Shekhar, A., Bockbrader, M.A., O'Donnell, B.F., 2005. Steady state visual evoked potential abnormalities in schizophrenia. Clin.Neurophysiol. 116, 614-624.

Lalor, E.C., De, S.P., Krakowski, M.I., Foxe, J.J., 2012. Visual sensory processing deficits in schizophrenia: is there anything to the magnocellular account? Schizophr.Res. 139, 246-252.

Lewis, D.A., Hashimoto, T., Volk, D.W., 2005. Cortical inhibitory neurons and schizophrenia. Nat.Rev.Neurosci. 6, 312-324.

Lindenmayer, J.P., Bernstein-Hyman, R., Grochowski, S., Bark, N., 1995. Psychopathology of Schizophrenia: initial validation of a 5-factor model. Psychopathology 28, 22-31.

Lorincz, M.L., Crunelli, V., Hughes, S.W., 2008. Cellular dynamics of cholinergically induced alpha (8-13 Hz) rhythms in sensory thalamic nuclei in vitro. J.Neurosci. 28, 660-671.

Maris, E., Oostenveld, R., 2007. Nonparametric statistical testing of EEG- and MEG-data. J.Neurosci.Methods 164, 177-190.

Maris, E. 2011. Statistical testing in electrophysiological studies. Psychophysiol. 49, 549-565.

Markov, N.T., Vezoli, J, Chameau, P., Falchier, A., Quilodran, R., Huissoud, C., Lamy, C., Misery, P., Giroud, P., Ullman, S. et al. 2014. Anatomy of hierarchy: feedforward and feedback pathways in macaque visual cortex. J.Comp.Neurol. 522, 225-259.

Michalareas, G., Vezoli, J., van Pelt, S., Schoffelen, J-M, Kennedy, H., Fries, P. 2016. Alpha-beta and Gamma Rhythms Subserve Feedback and Feedforward Influences among Human Visual Cortical Areas. Neuron 89, 1-14.

Mo, J., Schroeder, C.E., Ding, M., 2011. Attentional modulation of alpha oscillations in macaque inferotemporal cortex. J.Neurosci. 31, 878-882.

Muthukumaraswamy, S.D., Singh, K.D., Swettenham, J.B., Jones, D.K., 2010. Visual gamma oscillations and evoked responses: variability, repeatability and structural MRI correlates. Neuroimage 49, 3349-3357.

Muthukumaraswamy, S.D., Singh, K.D., 2013. Visual gamma oscillations: the effects of stimulus type, visual field coverage and stimulus motion on MEG and EEG recordings. Neuroimage 69, 223-230.

Oostenveld, R., Fries, P., Maris, E., Schoffelen, J.M., 2011. FieldTrip: Open source software for advanced analysis of MEG, EEG, and invasive electrophysiological data. Comput.Intell.Neurosci. 2011, 156869.

Philips, W.A., Silverstein, S.M. 2003. Convergence of biological and psychological perspectives on cognitive coordination in schizophrenia. Behav. Brain Sci. 26, 65-138.

Rivolta, D., Castellanos, N.P., Stawowsky, C., Helbling, S., Wibral, M., Grützner, C., Koethe, D., Birkner, K., Kranaster, L., Enning, F., Singer, W., Leweke, F.M., Uhlhaas, P.J., 2014. Source-reconstruction of event-related fields reveals

hyperfunction and hypofunction of cortical circuits in antipsychotic-naive, first-episode schizophrenia patients during Mooney face processing. J.Neurosci. 34, 5909-5917.

Rivolta, D., Heidegger, T., Scheller, B., Sauer, A., Schaum, M., Birkner, K., Singer, W., Wibral, M., Uhlhaas, P.J., 2015. Ketamine Dysregulates the Amplitude and Connectivity of High-Frequency Oscillations in Cortical-Subcortical Networks in Humans: Evidence From Resting-State Magnetoencephalography-Recordings. Schizophr.Bull. 41, 1105-1114.

Romei, V., Brodbeck, V., Michel, C., Amedi, A., Pascual-Leone, A., Thut, G., 2008. Spontaneous fluctuations in posterior alpha-band EEG activity reflect variability in excitability of human visual areas. Cereb.Cortex 18, 2010-2018.

Romei, V., Gross, J., Thut, G., 2010. On the role of prestimulus alpha rhythms over occipito-parietal areas in visual input regulation: correlation or causation? J.Neurosci. 30, 8692-8697.

Saalmann, Y.B., Pinsk, M.A., Wang, L., Li, X., Kastner, S., 2012. The pulvinar regulates information transmission between cortical areas based on attention demands. Science 337, 753-756.

Saß, H., Wittchen, H.U., Zuadig, M., Houben, I., 2003. *Diagnostisches und Statistisches Manual Psychischer Störungen - Textrevision - DSM-IV-TR*.Hogrefe, Göttingen.

Selemon, L.D., Rajkowska, G., Goldman-Rakic, P.S., 1995. Abnormally high neuronal density in the schizophrenic cortex. A morphometric analysis of prefrontal area 9 and occipital area 17. Arch.Gen.Psychiatry 52, 805-818.

Sohal, V.S., Zhang, F., Yizhar, O., Deisseroth, K., 2009. Parvalbumin neurons and gamma rhythms enhance cortical circuit performance. Nature 459, 698-702.

Spencer, K.M., Nestor, P.G., Perlmuller, R., Niznikiewicz, M.A., Klump, M.C., Frumin, M., Shenton, M.E., McCarley, R.W., 2004. Neural synchrony indexes disordered perception and cognition in schizophrenia. Proc.Nat.Acad.Sci.U.S.A. 101(49), 17288-17293.

Spencer, K.M., 2008. Visual gamma oscillations in schizophrenia: implications for understanding neural circuitry abnormalities. Clin.EEG.Neurosci. 39, 65-68.

Steriade, M., Gloor, P., Llinas, R.R., Lopes de Silva, F.H., Mesulam, M.M., 1990. Report of IFCN Committee on Basic Mechanisms. Basic mechanisms of cerebral rhythmic activities. Electroencephalogr.Clin.Neurophysiol. 76, 481-508.

Sun, L., Castellanos, N., Grützner, C., Koethe, D., Rivolta, D., Wibral, M., Kranaster, L., Singer, W., Leweke, M.F., Uhlhaas, P.J., 2013. Evidence for dysregulated high-frequency oscillations during sensory processing in medication-naive, first episode schizophrenia. Schizophr.Res. 150, 519-525.

Tan, H.R., Lana, L., Uhlhaas, P.J., 2013. High-frequency neural oscillations and visual processing deficits in schizophrenia. Front Psychol. 4, 621.

Thut, G., Nietzel, A., Brandt, S.A., Pascual-Leone, A., 2006. Alpha-band electroencephalographic activity over occipital cortex indexes visuospatial attention bias and predicts visual target detection. J.Neurosci. 26, 9494-9502.

Uhlhaas, P.J., Silverstein, S.M., 2005. Perceptual organization in schizophrenia spectrum disorders: empirical research and theoretical implications. Psychol.Bull. 131, 618-632.

Uhlhaas, P.J., Philips, W.A., Mitchell, G., Silverstein, S.M., 2006. Perceptual grouping in disorganized schizophrenia. Psychiatry Res. 145, 105-117.

Uhlhaas, P.J., Mishara, A.L., 2007. Perceptual anomalies in schizophrenia: integrating phenomenology and cognitive neuroscience. Schizophr.Bull. 33, 142-156.

Uhlhaas, P.J., Singer, W., 2012. Neuronal dynamics and neuropsychiatric disorders: toward a translational paradigm for dysfunctional large-scale networks. Neuron 75, 963-980.

van Dijk H., Schoffelen, J.M., Oostenveld, R., Jensen, O., 2008. Prestimulus oscillatory activity in the alpha band predicts visual discrimination ability. J.Neurosci. 28, 1816-1823.

van Kerkoerle, T., Self, M.W., Dagnino, B., Gariel-Mathis, M.A., Poort, J., van der, T.C., Roelfsema, P.R., 2014. Alpha and gamma oscillations characterize feedback and feedforward processing in monkey visual cortex. Proc.Natl.Acad.Sci.U.S.A 111, 14332-14341.

Villeneuve, M.Y., Thompson, B., Hess, R.F., Casanova, C., 2012. Pattern-motion selective responses in MT, MST and the pulvinar of humans. Eur.J.Neurosci. 36, 2849-2858.

Wang, X.J., Buzsaki, G., 1996. Gamma oscillation by synaptic inhibition in a hippocampal interneuronal network model. J.Neurosci. 16, 6402-6413.

Whittington, M.A., Traub, R.D., Jefferys, J.G., 1995. Synchronized oscillations in interneuron networks driven by metabotropic glutamate receptor activation. Nature 373, 612-615.

Whittington, M.A., Traub, R.D., 2003. Interneuron diversity series: inhibitory interneurons and network oscillations in vitro. Trends Neurosci. 26, 676-682.

Yoon, J.H., Maddock, R.J., Rokem, A., Silver, M.A., Minzenberg, M.J., Ragland, J.D., Carter, C.S., 2010. GABA concentration is reduced in visual cortex in schizophrenia and correlates with orientation-specific surround suppression. J.Neurosci. 30, 3777-3781.

Table 1

Demographic data and PANSS scores.

Demographic data			
	Nr Females (Total)	MEAN AGE	STDEV AGE
Schizophrenia	6 (16)	34	10.6
Healthy controls	6 (16)	31	8.0

PANSS scores Chronic Schizophrenia patients (n=15)		
	MEAN	STDEV
Negative	14	6.2
Excitement	7	2.9
Cognitive	10	2.7
Positive	10	3.8
Depression	11	2.6
Total	52	13.3

Abbreviations: STDEV = Standard deviation of the mean

Table 2

Statistical results of group differences in number of trials included in the MEG analyses, behavioural performance and individually estimated alpha- and gamma-peak frequencies.

	Healthy controls subjects (n = 16)		Schizophrenia subjects (n = 16)		Results of statistical analysis	
	mean	SEM	mean	SEM	*t*-value	*p*-value
Number of trials included	322	23.6	336	27.9	-0.37	0.71
Response time (milliseconds)	572	52	596	50	-0.34	0.74
Accuracy of detection (%)	94.7	1.0	82.5	3.1	3.72	0.001*
Alpha peak frequency (Hz)	10.4	0.2	9.5	0.4	2.14	0.04*
Gamma peak frequency (Hz)	58	1.4	56	1.8	0.63	0.53

Abbreviations: SEM = Standard Error of the Mean. Significant results are indicated with *.

Table 3

Statistical results of sensor-, source-, and virtual-channel analysis of group differences.

	Sensor-level analysis			Source-level analysis		
	p-value	frontal sensors	*p*-value	posterior sensors	*p*-value*	clusters
Alpha power						
250-750 ms	n.s.		n.s.		n.s.	
750-1250 ms	n.s.		n.s.		< 0.05	6
Gamma power						
250-750 ms	< 0.04	22	< 0.02	30	< 0.05	31
750-1250 ms	< 0.03	19	< 0.01	34	< 0.05	26

	Virtual channel analysis					
	Cuneus		Lingual Gyrus		Fusiform Gyrus	
	p-value	time	*p*-value	time	*p*-value	time
Alpha power	n.s.		n.s.		< 0.05	300-1600
Gamma power	n.s.		< 0.05	-50-1350	< 0.05	100-600

Abbreviations: n.s. = non significant, time = time-points (in ms) of significant group differences, * uncorrected for multiple comparisons (critical *t*-value = 2.13)

Table 4

Significant Spearman's *rho* correlations between behavioural performance, symptom severity (PANSS scores; Cognitive factor) and oscillatory activity in three virtual-channel ROIs.

Contrast		*rho*-values	*p*-values*
Behavioural accuracy	FUS-ALPHA-power	0.767	0.001
	LIN-ALPHA-power	0.763	0.001
	CUN-ALPHA-power	0.752	0.001
	FUS-GAMMA-power	0.770	0.001
	LIN-GAMMA-power	0.760	0.001
	CUN-GAMMA-power	0.724	0.002
PANSS-Cognitive	FUS-ALPHA-power	-0.618	0.014
	LIN-ALPHA-power	-0.605	0.017
	CUN-ALPHA-power	-0.545	0.036
	FUS-GAMMA-power	-0.611	0.016
	LIN-GAMMA-power	-0.565	0.028
	CUN-GAMMA-power	-0.463	0.083

Notes: * 2-tailed test, CUN = cuneus, FUS = fusiform gyrus, LIN = lingual gyrus, ALPHA (8-13 Hz), GAMMA (47-67 Hz), n = 15 ScZ patients

Figure Legends

Fig. 1. Experimental paradigm. Following a baseline period of 1.5 sec, participants were presented with an inward-moving concentric grating (second and third picture: arrows are added here to indicate the movement direction). This movement would speed up at a random time point between 0.5 and 3.0 sec after its onset and had to be detected and reported by button press. Visual feedback was given after each trial, shortly after the response terminated the stimulus presentation.

Fig. 2. Sensor-level results. (A) Time-frequency representations (TFRs) of absolute changes in power from baseline (-500-0 ms) for data averaged over 78 sensors located over the visual cortex (see red dots in ROI plot, panel C), separately for lower frequencies up to 35 Hz (top figures) and higher frequencies up to 90 Hz (bottom figures) as well as separately per group (HC's on the left, ScZ subjects on the right). (B) Topographical distributions (250-1250 ms post grating onset) of the ALPHA effect (8-13 Hz) and the GAMMA effect (47-67 Hz) for HC's on the left and ScZ subjects on the right. (C) FFT-based power changes across the frequency spectrum, shown for the same sensors as used for the TFRs in panel A, separately per group and baseline (-500-0 ms) and active window (500-1000 ms) averaged data. Shaded error bars represent standard error of the means (SEM) of the group of included subjects. (D) Cluster plot, highlighting sensors of significant frontal (light blue) and posterior (dark blue) gamma-power changes between groups. Because clusters were very stable over time, data shown is pooled over early and late time windows.

Fig. 3. Source-level results. (A) Source-reconstructions of early (250-750 ms) absolute change in gamma-band power (around individual peak frequency) from baseline (-500-0 ms), separately for healthy control subjects (left), schizophrenia patients (middle) and the

difference between ScZ and HC subjects (right). (B) As panel A, but for individually estimated alpha-peak centred activity. (C) Sagittal- and axial-view slices showing significant (uncorrected for MCP) clusters of activity related to the GAMMA effect (left; 250-750 ms) and ALPHA effect (right: 750-1250 ms). Critical *t*-value for acceptance of a significant cluster was ± 2.13.

Fig. 4. Virtual-channel analyses results. LCMV beamformer-reconstructed time-series of power changes and corresponding changes in statistical probabilities of significant group differences ($p < 0.05$) across time, shown for each of the three selected ROIs (averaged left and right Fusiform Gyrus [panel A], Lingual Gyrus [panel B], and Cuneus [panel C]; SPM coordinates are reported), separately for ALPHA (8-13 Hz) and GAMMA (47-67 Hz) band activity. Shaded error bars represent standard error of the means (SEM) of the group of included subjects. For clarity, significant group differences are additionally highlighted by grey boxes overlaying the statistical probability plots.

Fig. 5. Correlations: Scatterplots demonstrating significant correlations between behavioural accucary (left panel figures) and PANSS scores on the 'Cognitive factor' subscale (right panel figures) with ALPHA (8-13 Hz) and GAMMA (47-67 Hz) task-induced power changes (250-750 ms post stimulus onset) for the Fusiform Gyrus (top figures), Lingual Gyrus (middle figures), and Cuneus (lower figures). Data points include the 15 (out of 16) schizophrenia patients with available PANSS scores. * $p < 0.05$ (2-tailed), ** $p < 0.01$ (2-tailed).

Figure1: Experimental Paradigm

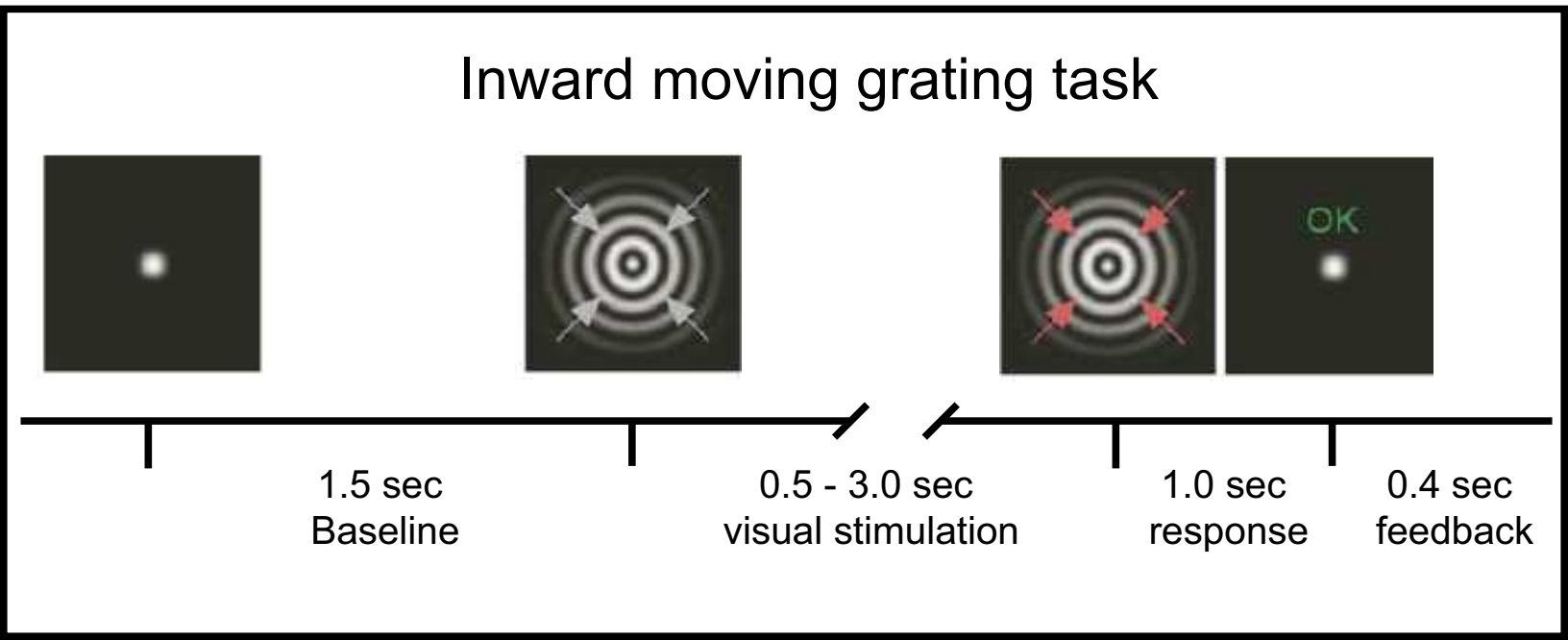

Figure2: Sensor-level results

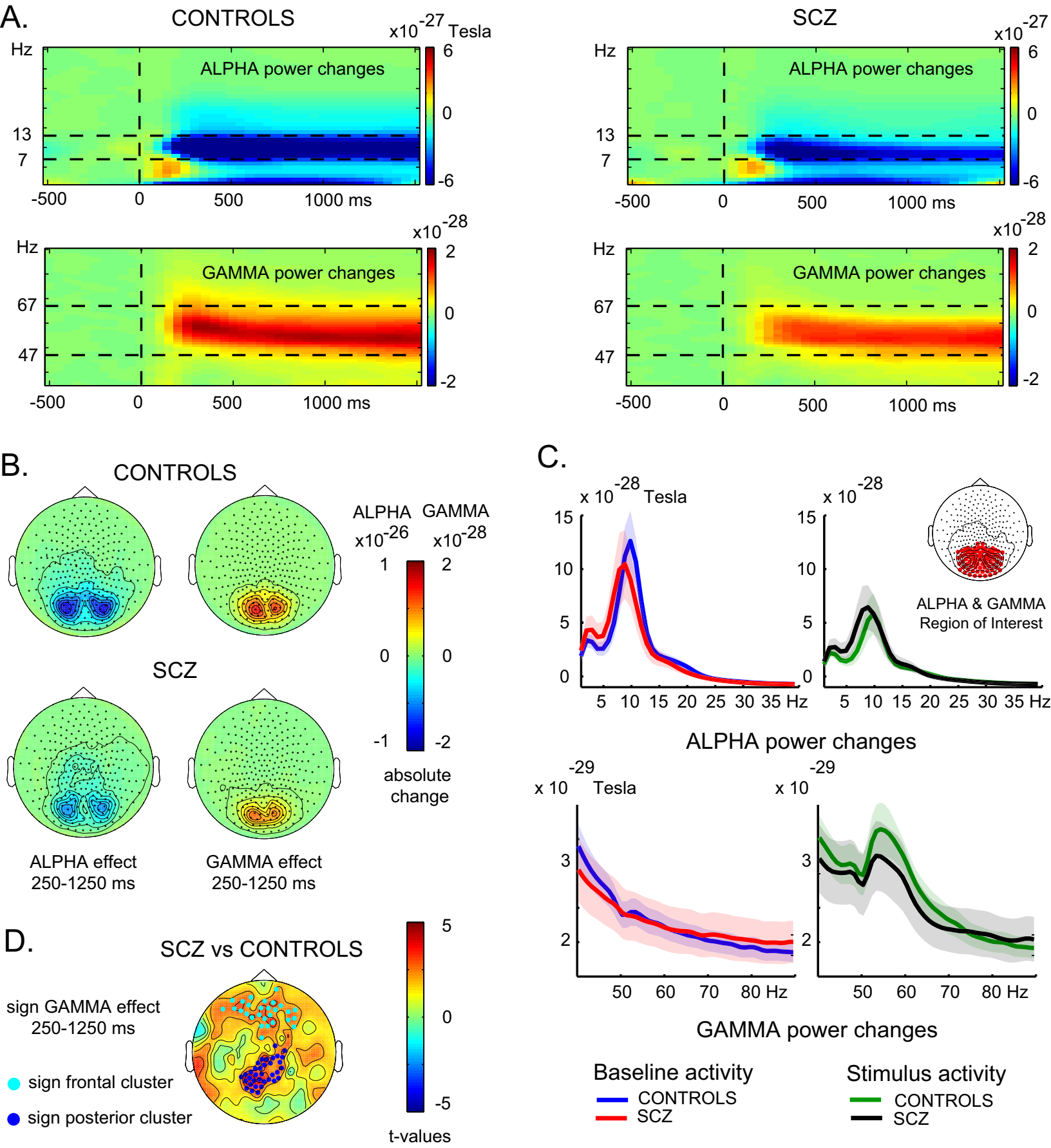

Figure3: Source-level results

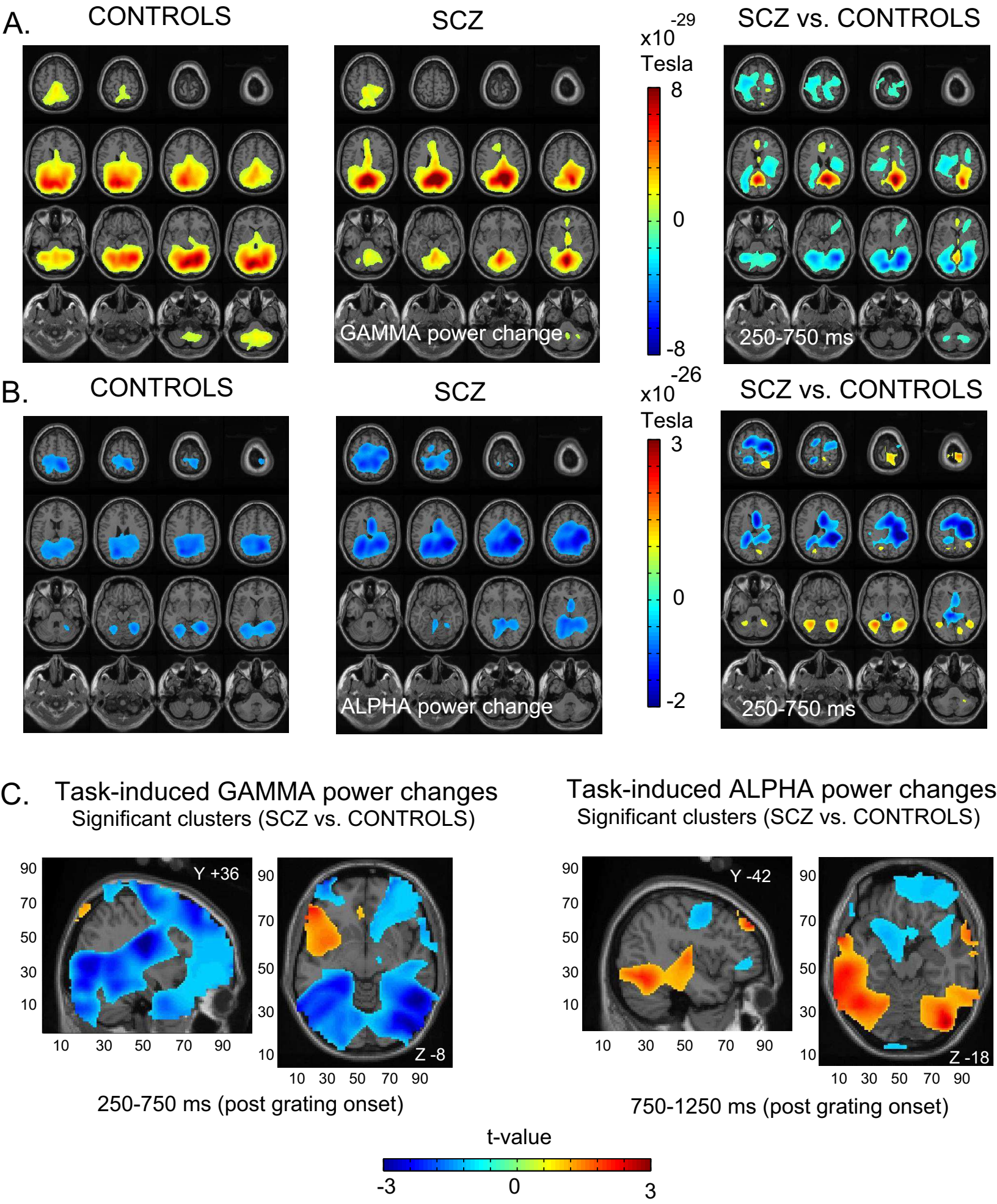

Figure4: Virtual channel analyses results

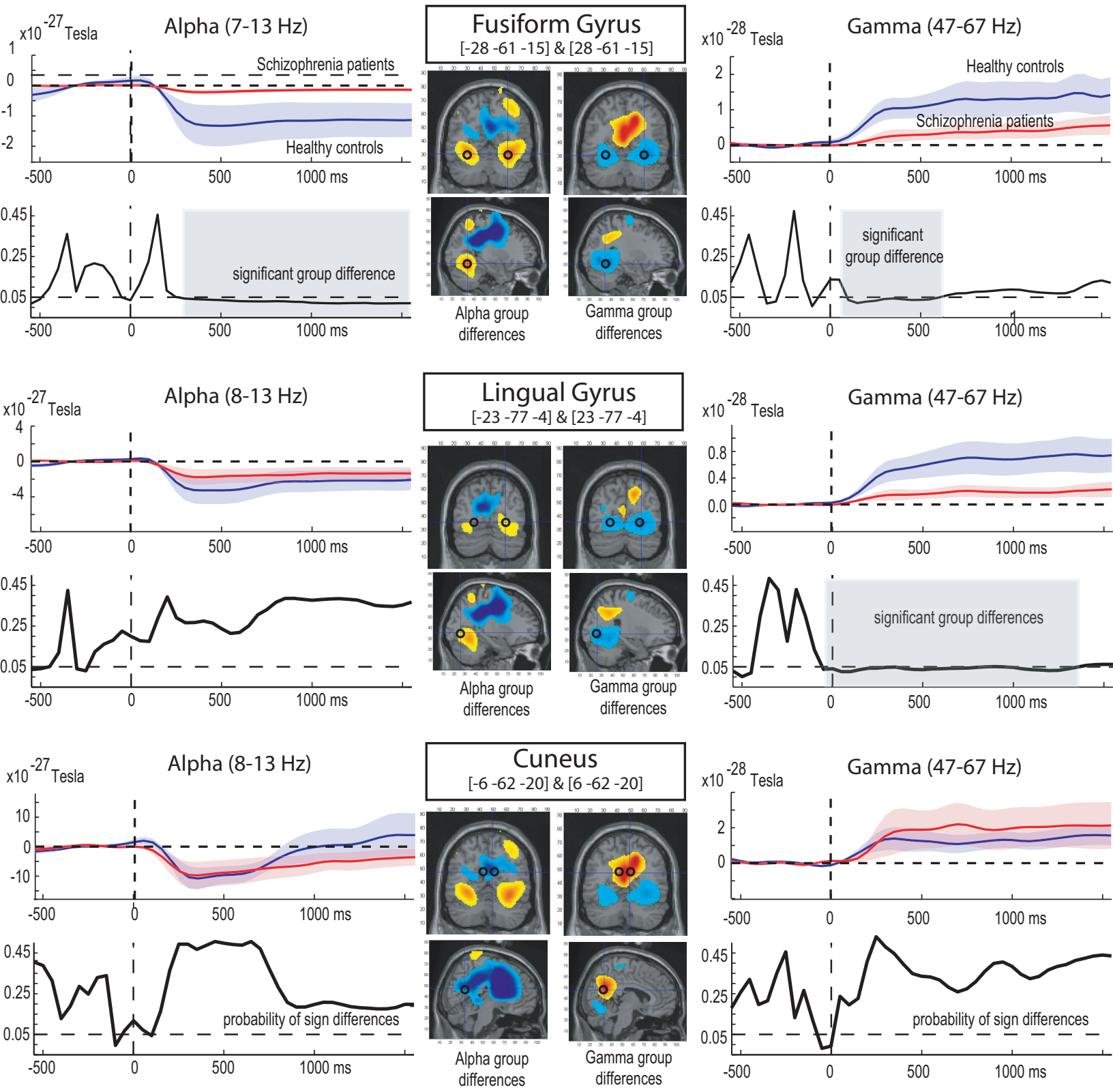

Figure5: Correlations

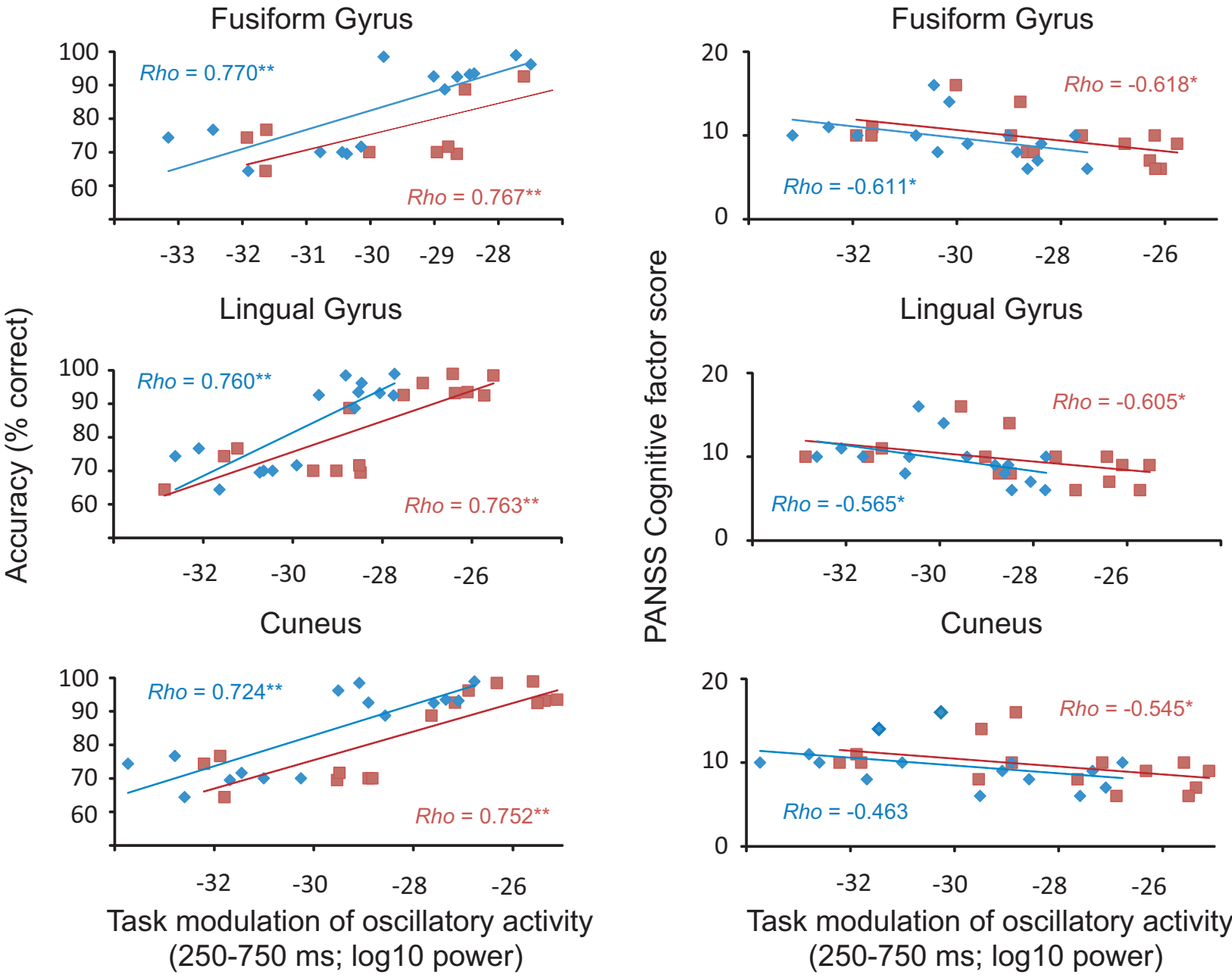

Acknowledgments: The authors declare no competing financial interests. Davide Rivolta was supported by the LOWE grant Neuronale Koordination Forschungsschwerpunkt Frankfurt (NeFF).

Conflict of Interest

On behalf of all authors, I declare that there are no known conflicts of interest associated with the publication and that there has been no significant financial support for this work that could have influenced its outcome. All authors have read and approved the manuscript prior to submission. Due consideration has been given to the protection of intellectual property associated with this work, following our institutional guidelines. Ethical approval of this study was obtained and is reported in the manuscript.

The corresponding author,

Tineke Grent-‘t-Jong

Contributors:

Tineke Grent-‘t-Jong contributed to analyses and write-up of the study.

Davide Rivolta contributed to design, recordings, analyses and write-up.

These two authors investigated equal amounts of work and time into the study and current manuscript and therefore *share first authorship*.

Andreas Sauer contributed to design and and recordings.

Michael Grube, Wolf Singer, Michael Wibral and Peter Uhlhaas (leading investigator) are senior scientists who supervised the entire study, from design to final submission.